



Published in final edited form as:

*Nanomedicine*. 2017 August ; 13(6): 1863–1867. doi:10.1016/j.nano.2017.04.003.

## Quantitative microscopy-based measurements of circulating nanoparticle concentration using microliter blood volumes

Gregory T. Tietjen, PhD<sup>a</sup>, Jenna DiRito<sup>a</sup>, Jordan S. Pober, MD, PhD<sup>b,1</sup>, W. Mark Saltzman, PhD<sup>a,\*</sup>,<sup>1</sup>

<sup>a</sup>Department of Biomedical Engineering, Yale University, New Haven, CT, USA

<sup>b</sup>Department of Immunobiology, Yale University, New Haven, CT, USA

### Abstract

Nanoparticles (NPs) are potential drug delivery vehicles for treatment of a broad range of diseases. Intravenous (IV) administration, the most common form of delivery, is relatively non-invasive and provides (in theory) access throughout the circulatory system. However, in practice, many IV injected NPs are quickly eliminated by specialized phagocytes in the liver and spleen. Consequently, new materials have been developed with the capacity to significantly extend the circulating half-life of IV administered NPs. Unfortunately, current procedures for measuring circulation half-lives are often expensive, time consuming, and can require large blood volumes that are not compatible with mouse models of disease. Here we describe a simple and reliable procedure for measuring circulation half-life utilizing quantitative microscopy. This method requires only 2  $\mu$ L of blood and minimal sample preparation, yet provides robust quantitative results.

### Keywords

Nanoparticles; Circulation half-life; Quantitative microscopy

---

Nanoparticles (NPs) have been used as drug delivery vehicles in a variety of therapeutic contexts from cancer to cardiovascular disease.<sup>1,2</sup> In many settings, duration of NP circulation may represent an important parameter, as accumulation at the site of need can require prolonged circulation.<sup>3</sup> This poses a challenge, given the efficiency with which the mononuclear phagocyte system can eliminate foreign bodies.<sup>4,5</sup> So called ‘stealth’ coatings [e.g. polyethylene glycol (PEG); hyperbranched glycerol], have been shown capable of prolonging circulation times.<sup>6–8</sup> Consequently, measurements of circulation half-life in relevant animal models can be essential to engineering therapeutic efficacy.<sup>9,10</sup>

For many diseases, murine models represent the most widely used and well-defined experimental systems.<sup>11</sup> However, the small blood volume of mice (typically ~2 mL)

---

\*Corresponding author at: Department of Biomedical Engineering, Yale University, New Haven, CT, 06525. mark.saltzman@yale.edu (W.M. Saltzman).

<sup>1</sup>These authors contributed equally.

Appendix A. Supplementary data

Supplementary data to this article can be found online at <http://dx.doi.org/10.1016/j.nano.2017.04.003>.

presents an obstacle for measuring NP circulation half-life. NIH guidelines stipulate that no more than 1% of blood volume should be removed per 24 h in mice.<sup>12</sup> This constitutes ~20  $\mu\text{L}$  across all sampling points (typically 8+), which limits the volume per sample to ~2–3  $\mu\text{L}$  when sampling from a single animal. Unfortunately, measuring the circulating concentration of NPs loaded with fluorescent dyes (the most common labeling method) typically requires ~10–20  $\mu\text{L}$  of blood per sample<sup>6,7</sup> or a specialized intravital imaging/analysis platform.<sup>13</sup>

Ideally, quantification of NP blood concentration in mice could be done in a 2  $\mu\text{L}$  volume and without need for additional processing or an expensive intravital imaging system. In principle, quantitative microscopy can be used to directly measure dye-loaded NP concentrations in small blood volumes smeared between a glass slide and coverslip. However, measuring a consistent fluorescent intensity for a given blood sample requires a reproducible path length (i.e. thickness) of the blood layer, assuming all other parameters remain constant (e.g. quantum yield, fluorophore concentration, incident light intensity, etc.).<sup>14</sup> The high viscosity of blood and static charge of glass have the potential to cause significant variation in how blood samples spread and thereby lead to significant path length variations within and between samples. Here we demonstrate that a second color reference NP, added after blood collection, can correct for these variations. Thus, referenced quantitative microscopy provides a robust and efficient method for measurement of circulating NP concentration.

## Methods

### Materials

PLA-PEG polymer (16–5 kDal MW) was purchased from PolySciTech (West Lafayette, IN) and used as received without further purification. Anhydrous DMSO, Dil and DiO stains, and Fisherbrand Superfrost Microscope Slides were purchased from Life Technologies (Carlsbad, CA). Heparinized Eppendorf tubes were purchased from Fisher Scientific (Suwanee, GA). Isoflurane was purchased from Sigma-Aldrich (St Louis, MO). 12 mm diameter circular cover slips were purchased from VWR (Radnor, PA).

### NP formulation

NP were prepared by a standard nanoprecipitation procedure. PLA-PEG was dissolved at an initial concentration of 100 mg/mL in DMSO and then diluted to the desired concentration for NP formulation (typically ~55 mg/mL for the ~165 nm NPs used in this study) along with addition of either Dil or DiO dye also dissolved in DMSO. NPs were loaded with Dil or DiO dye at a final wt dye/wt polymer ratio of 0.5%. The dye/polymer solution in DMSO was added drop wise to vigorously stirring sterile diH<sub>2</sub>O in batches of 200  $\mu\text{L}$  polymer/dye solution added to 1.3 mL of diH<sub>2</sub>O with identical repetitions performed to generate a full NP batch. NP were subsequently filtered through a 1.2  $\mu\text{m}$  cellulose acetate membrane (GE Healthcare Life Sciences - Whatman) filter to remove any free dye or polymer aggregates and then pooled. Typically, 8 small batches of ~11 mg polymer each were combined for a total pooled batch size of ~88 mg initial polymer weight. The pooled NP solutions were then transferred to a 12 mL volume 10,000 MWCO dialysis cassettes (Thermo Scientific -Slide-A-Lyzer) and dialyzed against 2 $\times$  exchanges of ~2.2 L of diH<sub>2</sub>O at room temperature to

remove excess DMSO. Following dialysis, NPs were aliquoted and snap frozen in liquid N<sub>2</sub>. One aliquot from each NP batch was lyophilized in a pre-weighed tube in order to determine the NP concentration. Standard NP concentration was typically ~5 mg/mL. NP batches were diluted to ~0.1 mg/mL and analyzed via dynamic light scattering (DLS) to confirm NP size and homogeneity.

### Sample collection/preparation

All animal procedures were performed in accordance with the guidelines and policies of the Yale Animal Resource Center (YARC) and approved by the Institutional Animal Care and Use Committee (IACUC). Female C.B.-17 Scid/bg mice (13 animals; Charles River Laboratories) were used. Surgical procedures were performed using standard sterile surgical techniques. Blood samples were collected via tail nick with a sterile blade followed by collection with a p10 pipette. Typical collection volumes were 2 pL for quantitative microscopy or 12 µL for combined quantitative microscopy and microplate read. Once the blood volume was obtained, a sterile gauze was applied with pressure to stop any blood flow. The blood sample was promptly mixed 1:1 with 200 µg/mL DiO-NPs prealiquoted in a heparinized epitube (Fisher Scientific) by vigorous pipetting. Samples were then snap froze using liquid nitrogen and stored at -80 °C until analysis. After thawing, 2 µL of the blood/reference solution was spotted onto the untreated side of a glass slide and covered with a 12 mm diameter circular cover slip. Care was taken to ensure no air bubbles were caught under the coverslip. The standard was prepared via serial dilutions in blood, with a 5.1 mg/mL stock solution of Dil-NP, that yielded final concentrations ranging from 50 to 350 µg/mL. Samples were then diluted 1:1 with a 200 µg/mL solution of DiO-NP in DPBS. All samples were immediately imaged after coverslip application.

### Quantitative microscopy and data analysis

Images were collected using a Semrock GFP-1828A bandpass filter set (Ex: 470–495 nm; Em: 505–535 nm) and a Chroma TRITC/DU/CY3 filter set (Ex: 525–550 nm; Em: 580–630 nm) at 500 ms exposure with an air immersion apochromatic 20× objective (NA 1.4; Olympus) on an Olympus Z71 inverted microscope illuminated by an LED light source (Olympus L300) with each LED at full illumination intensity. These filter sets and illumination setup ensured no spectral bleed with these NPs which is a prerequisite for implementation of this technique (Supplemental Figure 1). Images were captured by an Olympus Retiga R6 CCD camera. For intensity quantification, the full-image mean intensity was calculated in ImageJ and then the background (from an identically prepared sample with blood only) was subtracted.

To ensure minimal photobleaching, we initially focused the sample via brightfield imaging to find the glass coverslip surface; this could be done at the edge of the coverslip to come within rough proximity of the fluorescence focal plane. From this point the image focus was fine-tuned using the reference DiO channel with care taken to minimize the amount of exposure. Once the proper focal plane was identified, the region of imaging was translated using a motorized stage to a fresh region that had not received any illumination. Each region was imaged only once followed by a raster-style translation to a fresh region. Prior to

imaging, the sample staged was leveled using optical focus to ensure that the translation did not affect the image focus.

The microscopy linear standard was prepared by adding serial dilutions of NPs at known concentrations to freshly collected blood (in a heparinized epitube). Fitting was done using linear regression with no constraints in Graph Pad Prism. The resultant slope (DilrDiO intensity ratio versus Dil-NP concentration in blood; y intercept was typically 0 as expected if there is no spectral bleed between NPs) was used to calculate absolute values of circulating NP concentration where desired by multiplying the best-fit slope value by the ratio of DiI:DiO mean intensities (after background subtraction) for a given image. Note that a strongly linear standard and a y-intercept of zero are both prerequisites for applying the approach described here to any given microscopy setup.

Half-life measurements were evaluated using the % of NP remaining referenced to the circulating concentration in the same animal measured at 2 m. The data were fit to a bi-exponential curve in GraphPad Prism with no constraints.

### **Blood collection and NP administration**

Mice were anesthetized via a bell jar induction method using a 70:30% propylene glycol:isoflurane mixture. 2 mL of the anesthetizing agent was added to a piece of sterile gauze which was placed under a plastic, inverted weigh boat with perforations that allow for ventilation of the isoflurane in the enclosed space and to ensure that the mice would not have direct contact with the isoflurane mixture. Mice were placed inside of the bell jar and respirations were closely monitored until they decreased to one respiration per second. Mice were then extracted from the jar and the retro-orbital injection or bleed was performed. Rear foot reflexes were tested using a toe pinch to ensure that the animals were properly anesthetized prior to injection/bleed. Approximately 100  $\mu$ L of blood was drawn retro-orbitally via capillary tubes pre-coated with heparin for standard preparation. For measurement of circulation half-life, nanoparticles were administered via retro-orbital injection using a 27-gauge needle. The standard injected volume was 100  $\mu$ L of 4.1 mg/mL Dil-NPs. For the full circulation half-life measurement, samples were collected at 2 m, 15 m, 30 m, 1 h, 2 h, 4 h, 10 h, 24 h, and 48 h time points.

### **Microplate analysis**

Microplate samples used a 10  $\mu$ L blood volume diluted to 100  $\mu$ L with DPBS in a 96 well clear bottom plate (Coming; Kennebunk, ME) read on a SpectraMax M5 (Molecular Devices; Sunnyvale, CA) microplate reader with 488/530 excitation/ emission for DiO NPs and 530/570 excitation/emission for Dil NPs with auto cutoff used for both. A standard confirmed a roughly similar level of sensitivity with this approach compared to the quantitative microscopy approach (Supplemental Figure 2).

### **Calculation of circulating NP concentration**

The mouse blood volume was extrapolated from the animal mass using an online calculator: <http://encorbio.com/protocols/Blood.htm>. Circulating concentration was then determined by

dividing the specific NP mass delivered (as determined by the known concentration of the NP solution and the volume delivered by retro-orbital injection) by this total volume.

## Results

### Reference NP corrects for heterogeneity within and between samples

We first assessed if quantitative microscopy could yield consistent fluorescence intensity for dye-loaded NPs in small blood volumes (2  $\mu\text{L}$ ). A mouse was injected retro-orbitally with 165 nm PLA—PEG (poly-lactic acid—poly-ethylene glycol) NPs loaded with Dil (1,1'-dioctadecyl-3,3,3',3'-tetramethylindocarbocyanine perchlorate) dye. Three hours after injection, 5 $\times$  blood samples were collected (2  $\mu\text{L}$  each by tail nick) in quick succession to ensure each was sampled from the same circulating concentration. Samples were immediately combined with 2  $\mu\text{L}$  of a reference solution containing 200  $\mu\text{g}/\text{mL}$  DiO (3,3'-dioctadecyloxycarbocyanine perchlorate)-loaded PLA—PEG NPs (for path length correction). Samples were subsequently spotted on glass slides and coverslipped, for imaging by quantitative microscopy.

As expected, intensity varied significantly across all levels of analysis (i.e. within a single image, between images of a single sample and between sdbd preparations; Figure 1). However, in all cases, referencing to DiO-NPs corrected this variability. Within a single image, NPs of both colors showed identical patterns of distribution (Figure 1, A). Single-color NP controls confirmed the absence of any spectral bleed between image channels (Supplemental Figure 1). Images collected within the same sample had highly variable mean intensities, likely due to uneven sample spreading (Figure 1, B). Referencing significantly reduced the relative standard deviation from 18.9% to 3.3% (as % of mean; Figure 1, C). Finally, prior to referencing, the mean sample intensity was as much as 4.75 $\times$  brighter in the brightest (sample #3) compared to the dimmest (sample #4) sample, again likely due to blood spreading variations (Figure 1, D). Nevertheless, NP referencing provided robust reduction in relative standard deviation between samples from 43.6% to 8.0% (5.5 $\times$  improvement).

### Quantitative microscopy recapitulates expected concentration in vivo

To confirm the reliability of our quantitative approach, we next generated a standard curve. Dil-NPs at known concentrations were titrated with a fixed volume dilution (1:1) in freshly collected mouse blood containing reference DiO-NPs and imaged. While intensity did trend higher with increasing NP concentration, the substantial variability yielded a poor linear fit ( $R^2 = 0.704$ ; Figure 2, A). However, referencing significantly reduced the data spread and substantially improved the linear fit ( $R^2 = 0.968$ ; Figure 2, B). Notably, the fit went through the origin (y-intercept =  $-0.02 \pm 1.0$ ;  $\pm = 95\%$  confidence) confirming the absence of any spectral bleed or other non-linear artifacts.

This standard curve was used to measure an expected concentration of NPs sampled from mouse blood after IV NP injection. Thirteen mice were administered  $\sim 100 \mu\text{L}$  of 4.1 mg/mL Dil-NPs resulting in a range of initial circulating concentrations depending on animal mass (varied from 16 to 30 g). After 2 min, to allow NP concentration to normalize, 2  $\mu\text{L}$  blood

samples were collected and analyzed by quantitative microscopy. The measured circulating concentration was generally within error of the expected concentration across all mice tested demonstrating the robustness of our approach (Figure 2, B).

### Circulation half-life measured by quantitative microscopy

We next compared our approach to a standard large-volume method using a microplate reader with 10  $\mu\text{L}$  of blood diluted in 90  $\mu\text{L}$  of DPBS. Six mice injected with  $\sim 100 \mu\text{L}$  of 4.1 mg/mL Dil-NPs were bled by tail nick at 2 min and again at 4.5 h with sufficient blood collected to allow for assay by both microplate and microscopy-based approaches (12  $\mu\text{L}$  total). The signal at 4.5 h was normalized to that at 2 min to assess the correspondence of the two methods in measuring the relative loss of NP from circulation (Figure 3, A). The measurements were quite consistent with an average difference of  $0.5\% \pm 3.4\%$  ( $\pm$  represents S.D.) between paired microscopy/microplate measurements (within the same mouse). Moreover, the average value derived from all six measurements were essentially identical between the two methods (microscopy — 39.8% of initial dose; microplate — 39.4%; Figure 3, A).

Finally, we measured the circulation half-life of PLA—PEG NPs in a cohort of 3 C.B.-17 Scid/Bg mice. Blood samples (2  $\mu\text{L}$ ) were drawn at various time points after NP injection (2, 15, 30, 60 min, 2, 4, 10, 24, 48 h). Due to the small volumes, all 9 samples could be collected within a single animal. Fitting the curve to a bi-exponential equation yielded a slow exponential decay rate of 4.6 h (95% confidence interval of 4.0 to 5.5 h; all other fit parameters in Supplementary Table 1). Notably, our microscopy based half-life curve overlapped with the microplate-based measurements (Figure 3, B and C). This half-life was also reasonably consistent with previous measurements of similar PLA—PEG NPs in different mouse strains.<sup>6</sup>

## Discussion

The modularity of NP drug carriers suggests significant therapeutic potential, particularly in an era of increasing personalization of medicine.<sup>15,16</sup> Developing tailored nanomedicines for specific applications will require diagnostic assays capable of increasingly sensitive quantification. In addition, personalization of NPs will require more detailed pharmacokinetic analysis that explores the full range of relevant parameters (e.g. size, surface-ligand density). Measuring circulation half-life as a function of a wide range of parameters has to date not been feasible in most instances. However, the quantitative microscopy approach developed here, significantly reduces the complexity of these measurements making detailed studies of the variables effecting pharmacokinetics much more tractable.

In addition to providing a more effective diagnostic tool, our approach also demonstrates the utility of quantitative microscopy. While fluorescence microscopy is frequently used as a qualitative tool in biology, quantitative applications are less common. Our work demonstrates that fluorescence microscopy has significant quantitative potential, particular under constraints of small  $\mu\text{L}$ -scale volumes. Ensuring robustness requires an understanding of how to correct for potential issues, but these corrections can be as simple as adding a

referencing color. As long as the proper controls are established, quantitative microscopy has significant untapped potential for the refinement of drug delivery vehicles.

## Supplementary Material

Refer to Web version on PubMed Central for supplementary material.

## Acknowledgments

Funding sources: This work was supported by the NIAID under T32 training grant AI089704, NHLBI under F32 fellowship grant HL131270, and a grant from AbbVie (YAP-12-2014).

## References

1. Wang AZ, Langer R, Farokhzad OC. Nanoparticle delivery of cancer drugs. *Annu Rev Med* 2012;63:185–98. [PubMed: 21888516]
2. Rhee JW, Wu JC. Advances in nanotechnology for the management of coronary artery disease. *Trends Cardiovasc Med* 2013;23:39–45. [PubMed: 23245913]
3. Blanco E, Shen H, Ferrari M. Principles of nanoparticle design for overcoming biological barriers to drug delivery. *Nat Biotechnol* 2015;33:941–51. [PubMed: 26348965]
4. Moghimi SM, Hunter AC, Murray JC. Long-circulating and targetspecific nanoparticles: theory to practice. *Pharmacol Rev* 2001;53:283–318. [PubMed: 11356986]
5. Moghimi SM, Szebeni J. Stealth liposomes and long circulating nanoparticles: critical issues in pharmacokinetics, opsonization and protein-binding properties. *Prog Lipid Res* 2003;42:463–78. [PubMed: 14559067]
6. Deng Y, Saucier-Sawyer JK, Hoimes CJ, Zhang J, Seo YE, Andrejcsk JW, et al. The effect of hyperbranched polyglycerol coatings on drug delivery using degradable polymer nanoparticles. *Biomaterials* 2014;35:6595–602. [PubMed: 24816286]
7. Peracchia MT, Fattal E, Desmaele D, Besnard M, Noel JP, Gomis JM, et al. Stealth PEGylated polycyanoacrylate nanoparticles for intravenous administration and splenic targeting. *J Control Release* 1999;60:121–8. [PubMed: 10370176]
8. Garcia KP, Zarschler K, Barbaro L, Barreto JA, O'Malley W, Spiccia L, et al. Zwitterionic-coated “stealth” nanoparticles for biomedical applications: recent advances in countering biomolecular corona formation and uptake by the mononuclear phagocyte system. *Small* 2014;10:2516–29. [PubMed: 24687857]
9. Zhu MT, Perrett S, Nie GJ. Understanding the particokinetics of engineered nanomaterials for safe and effective therapeutic applications. *Small* 2013;9:1619–34. [PubMed: 23225644]
10. Kamaly N, Xiao ZY, Valencia PM, Radovic-Moreno AF, Farokhzad OC. Targeted polymeric therapeutic nanoparticles: design, development and clinical translation. *Chem Soc Rev* 2012;41:2971–3010. [PubMed: 22388185]
11. Rosenthal N, Brown S. The mouse ascending: perspectives for human-disease models. *Nat Cell Biol* 2007;9:993–9. [PubMed: 17762889]
12. N. I. R. P. O. o. A. C. a. Use Guidelines for survival bleeding of mice and rats; 2015.
13. Jones SW, Roberts RA, Robbins GR, Perry JL, Kai MP, Chen K, et al. Nanoparticle clearance is governed by Th1/Th2 immunity and strain background. *J Clin Invest* 2013;123:3061–73. [PubMed: 23778144]
14. Hecht E. *Optics*, Addison-Wesley, Reading, Mass; 2002.
15. Tietjen GT, Saltzman WM. Nanomedicine gets personal. *Sci Transl Med* 2015;7.
16. Cheng CJ, Tietjen GT, Saucier-Sawyer JK, Saltzman WM. A holistic approach to targeting disease with polymeric nanoparticles. *Nat Rev Drug Discov* 2015;14:239–7. [PubMed: 25598505]

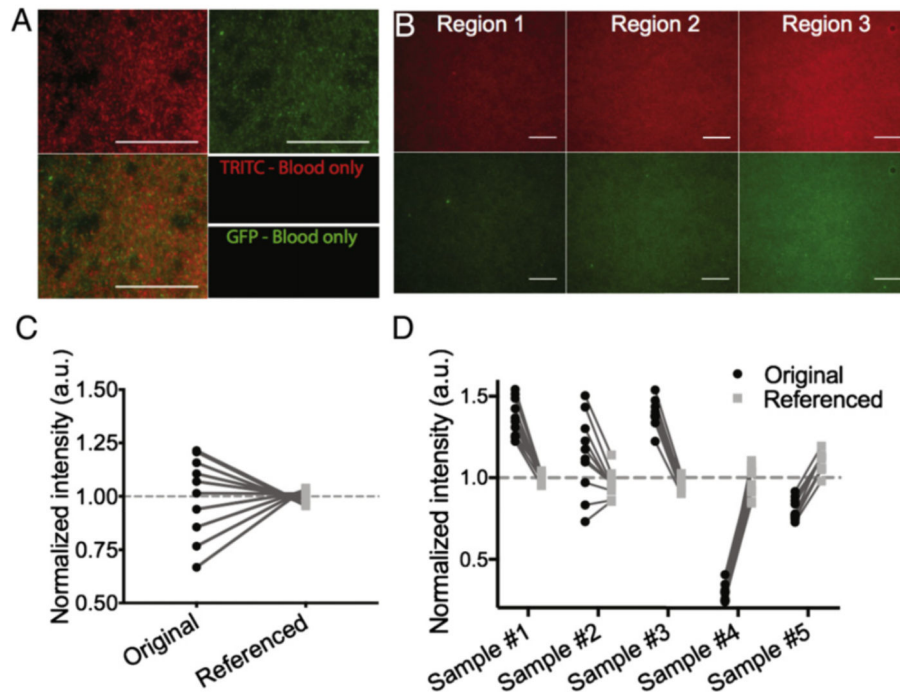


**Figure 1. Reference NP corrects for heterogeneity within and between samples**

(A) Representative images of Dil (red) and DiO (green) NPs demonstrating co-localization (overlay). (B) Independent regions within one sample showing varying intensity of Dil (top) and corresponding DiO-NP (bottom) images. Quantification of mean intensity for: (C) single sample of Dil-NP at 50 pg/mL or (D) 5 simultaneously collected samples from a single mouse before (black circles) and after referencing (gray squares); lines connect identical images. Values are normalized to the mean of their respective group (referenced or unreferenced). Scale bars represent 100  $\mu\text{m}$ .



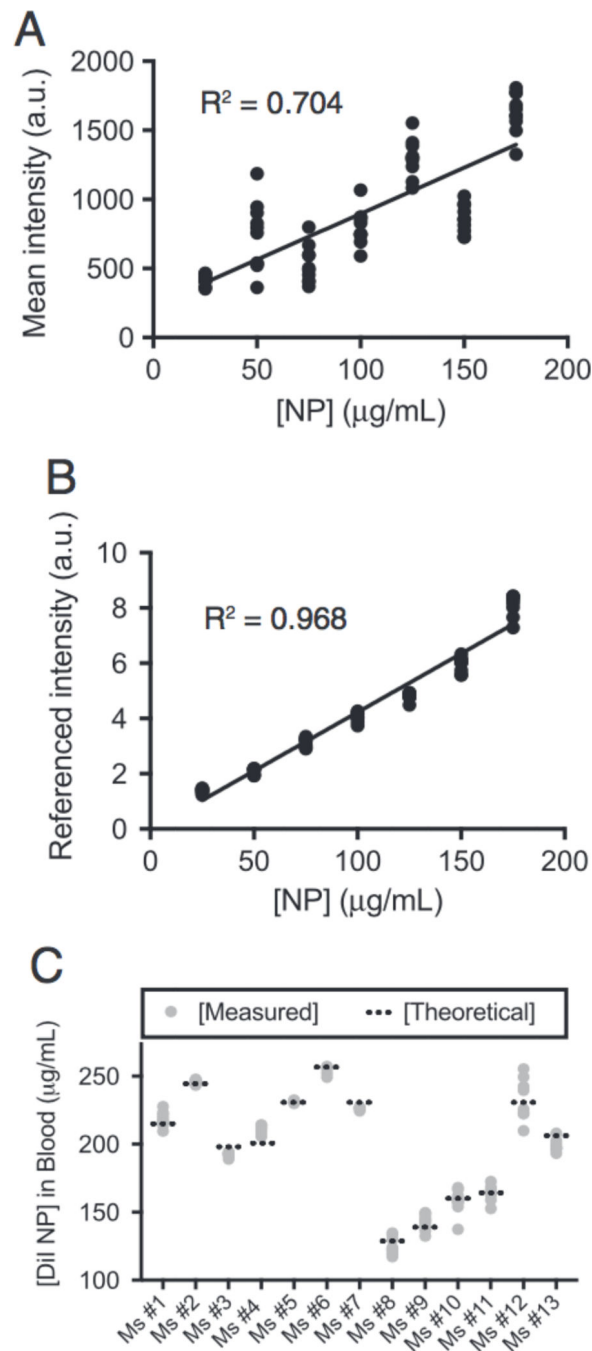


**Figure 2. Quantitative microscopy recapitulates expected concentration in vivo**  
 Unreferenced (**A**) and referenced (**B**) standard of Dil-NPs. Each data point represents an individual image; line represents linear fit. (**C**) Quantification of circulating NP concentration 2 min after injection; each gray dot represents an individual image (10 $\times$  per mouse). Theoretical values (dashed line) were calculated by amount of NP administered divided by mouse blood volume (from animal mass).

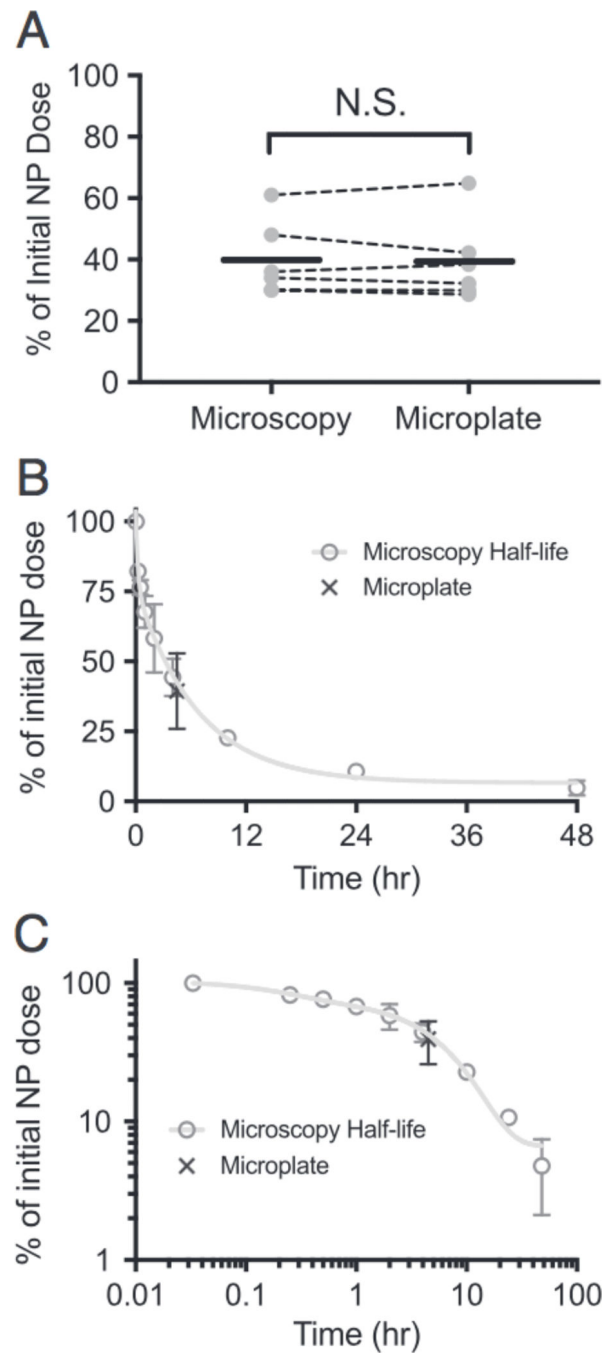


**Figure 3. Circulation half-life measured by quantitative microscopy**

(A) Percentage of NPs remaining 4.5 h after injection determined by referenced microscopy or microplate. Dashed lines connect samples from the same animal. Solid black line depicts mean for 6 animals. (B, C) Circulation half-life measured by referenced microscopy (gray circles) displayed on a linear (B) and log/log plot (C). Line through data shows fit to a bi-exponential curve. Black X depicts value measured for microplate from panel A. All error bars represent standard deviation.